# TrimBot2020 Deliverable D2.3

# Evaluation manipulator and tools version 1, running Open-Loop Motion Planning

Principal Author: Wageningen Research (WR) &
Wageningen University (WU)
Dissemination: CO

**Abstract**

Deliverable 2.3 is an evaluation deliverable, in which the open-loop trimming motion planning of the stationary robotic manipulator and the boxwood bush trimming end-effector quality are evaluated. Furthermore, an evaluation of the rose clipping end-effector is performed.

This document describes the objectives and methodologies for the quality assessment and presents quantitative and qualitative results of the evaluation tests; furthermore, in the result discussions, indications for following steps of the research are given.

Bush trimming evaluation test rig and the set of boxwood bushes used for the evaluation are illustrated together with the method for the analysis.

The results of bush trimming gave that, on average, 82% of total outgrowth was trimmed, of which only 51% of the trimming performance had a precision of higher than 20 mm.

The evaluation test for rose clipping showed that in 96% of the test positions the end-effector was able to cut, 75% of these locations were reached without any limitations in orientation or position.

In conclusion, the trimming open-loop performance was lower than the requirements, however, from the qualitative analysis of problems encountered during these tests, there is space for improvement. A redesign of the camera set-up and a refinement of the vision pipeline are necessary steps for the a better performance of the motion planning. Furthermore a more realistic requirement for the trimming precision has to be formulated.

The rose clipping end-effector had qualitative good performance. Furthermore since the tests were only attempted from one position, the performance can improve using multiple base displacement around the rose bushes.

Deliverable due: Month 24

 

# Contents



 

# 1 Introduction

In this deliverable, the performance of the first version end-effectors for bush-and-hedges trimming and rose clipping are evaluated. The procedure and test set-up to evaluate the bush trimming robot performance are given. Furthermore, the evaluation procedure of the rose clipping end-effector is described.

The stationary manipulator set-up and boxwood trimming end-effector were already described in Deliverable 2.2[1]. For the boxwood bush trimming test, a set of five bushes in pots were autonomously trimmed. For each bush a sequence of images was acquired before and after the trimming (Section 2.1.6).

For the rose clipping tool, 25 branches from a set of rose bushes were cut using the tool, described in Deliverable 2.1[5], mounted on the manipulator. The manipulator was controlled manually using a joystick.

From the project specifications given in the Deliverable 7.3[6] the trimming end-effector applied to boxwood bushes has to be able to cut surfaces with a precision higher than 5 mm and it has to be able to trim 95% of the outgrown branches. For rose clipping quantitative tests were performed to evaluate the quality of branch cutting (Section 3.1.3) and the buds reachability of a set of four rose bushes located in the test garden of Wageningen University & Research.

Main purpose of the document is to give a quantitative evaluation of the bush trimming performance and qualitative assessment of the rose clipping end-effector.

# 2 Bush Trimming Test

## 2.1 Materials and Methods

### 2.1.1 Bush Trimming Test Rig

The custom test rig that was described in Deliverable 2.2[1] was used. To simulate the test rig displacement around the bush a turntable by Shenzhen ComXim Technologies Co. was used (see Figure 1) (see Section 2.1.4).

The bushes were trimmed using open loop motion planning i.e. no feedback about the pose variation of a bush was calculated during the trimming process. Only an initial position was supplied to the motion planning by the vision system (see Deliverable 2.2 [1]). The robotic arm base was fixed at a distance of 78 cm from the center of the turntable. The bushes were trimmed on the turntable (see Figure 1). Each bush was rotated 72° five times, to simulate five displacements of the test rig around the bush.

 

Figure 1: Custom test rig with laptop, Pokini and Monitor (left). Kinova Jaco$^2$ robot arm mounted on the test rig; bush trimming end-effector and turntable (right).

### 2.1.2 Bush Trimming End-Effector

In Deliverable 2.2[1], a custom end-effector was shown using contra-rotating blades with long saw teeth of a particular shape, that can easily catch the boxwood branches between them (see Figure 2). Based on Deliverable 2.2[1], we designed and built a new end effector with a smaller and lighter motor to improve the robot dexterity.

The end-effector with the stereo camera is shown in Figure 3.

The rotation speed of the cutting blades was chosen taking into consideration the cut quality together with power consumption. The speed resultant due to sum of cutting blades rotation speed and end-effector motion speed is essential for the branch cut quality: too low speed of the contra-rotating blades implies that the branches are pulled during the cutting action resulting in a jagged cut; too high speed means that the branches are not clipped between the teeth of the blades but only pushed down. The rotation speed should be taken as low as possible to preserve the power of the on-board batteries. The speed of the cutting blades was fixed to 180 rpm.

### 2.1.3 Bush Set

Five spherical boxwood bushes, with a diameter of approximatively 30 cm, were used for the trimming test, Figure 4. The bushes were labeled with a code to identify each bush before and after the trimming. They were not trimmed for several weeks and then the grown branches were measured.

 

Figure 2: Improved design of custom bush trimming end-effector with smaller motor

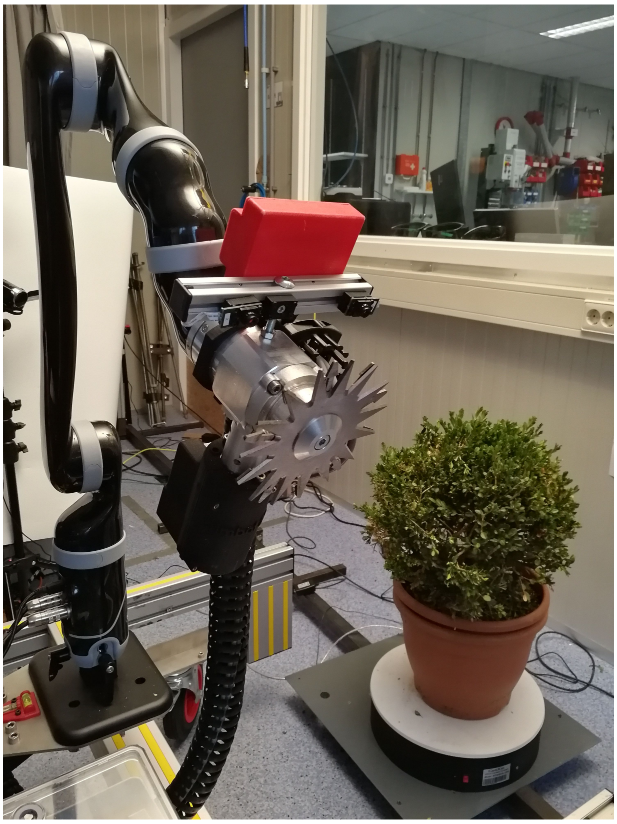

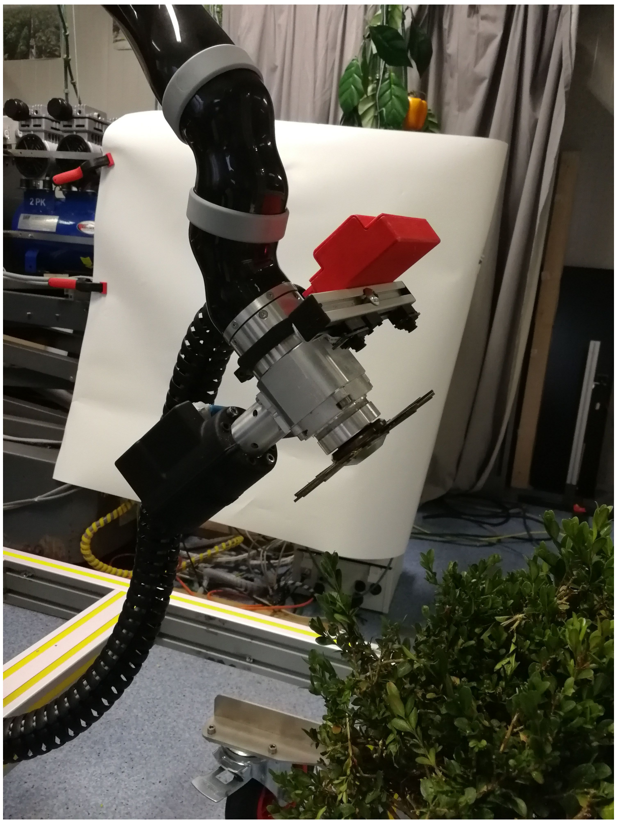

Figure 3: Custom bush trimming end-effector with stereo camera. Front view (left) and lateral view (right)

The measurements revealed that the new outgrowth was between the 5 and 15 cm following an anisotropic growth model, Figure 4. From the project specifications trimming end-effector has to be

 


Figure 4: Set of bushes for the evaluation(center-up) and bush number 3 labeled (left-down). Example of anisotropic growth (right-down)

 

able to trim bush branches that overgrown up to 40 mm from the desired shape without jamming. Branches longer than 12 cm where pruned back manually by 50%, in order to stay close to the specifications of Deliverable 7.3[6].

The goal was to trim the bushes back to the original diameter, maintaining their spherical shape.

### 2.1.4 Bush Trimming Evaluation Rig

Figure 5: Evaluation rig (left); turntable with back light (right).

The performance was evaluated using a method of extrapolating the bush profiles using a sequence of silhouettes[2] for each bush. For each bush two sequences of silhouettes were acquired: one before the trimming test and one after.

Using the evaluation rig with a back light projection on a white reflecting screen (see Figure 5), a sequence of pictures was acquired. In this way the profile of the bush was defined by a straightforward segmentation. Using the ComXim Technologies Co. turntable (Section 2.1.1), each bush was rotated 360° acquiring a evaluation image each degree. For the image acquisition, MVTec HALCON 13 software for machine vision (see Section 2.1.5) was used.

A black and white Prosilica GC 2450 camera, 2448 $\times$ 2050 pixels resolution, equipped with a 25 mm lens was mounted at 4 meter distance from the turntable to acquire a picture of the whole bush with minimal external edge occlusion due to the pinhole camera model effect. The lens distortion was corrected using a calibration pattern and the correction procedure of HALCON 13.

 

### 2.1.5 Evaluation Software

To acquire and to analyze the bush pictures we used HALCON 13 by MVTec as development tool. MVTec HALCON is the comprehensive standard software for machine vision with an integrated development environment.

Each picture was segmented by thresholding its gray intensity level (see Figure 6 ) to extract the bush silhouette. Then the pot was automatically detected and the bush extrapolated.

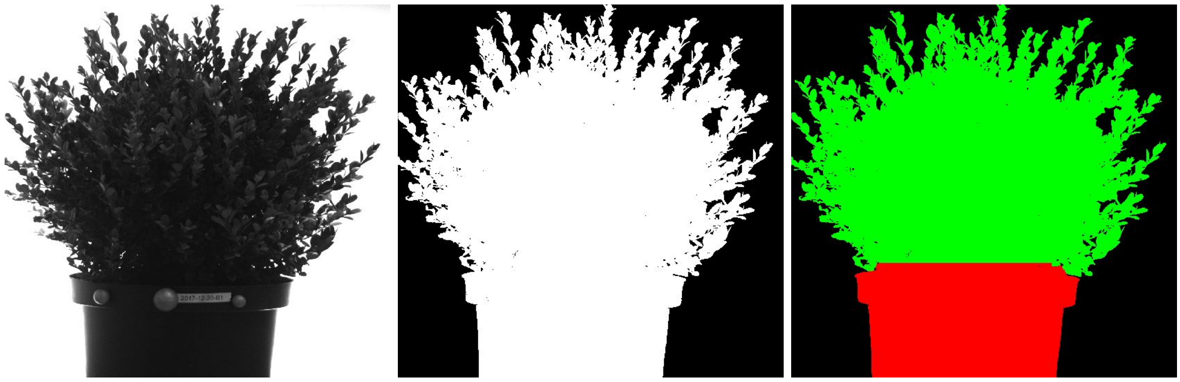

Figure 6: Raw image (left); binary image (center); pot and bush detection (right)

**Image Registration** To determine the correspondence between each bush image before and after the trimming we registered the images using landmarks. Due to the intrinsic high precision of the turntable ($\pm$ 0.1°) the number of landmarks could be limited to only three. Three reflecting spheres with diameters of 30 mm, 20 mm, and 15 mm were mounted on the pot edge of each bush. Segmenting the images on these landmarks we used a block match registration to find the corresponding image of the bush before and after the trimming for the initial rotation angle of the bush.

Using Normalized Cross Correlation (NCC) rigid registration, the corresponding image of the bush before and after the trimming for the initial rotation angle of the bush could be found (see Figure 7). In this way, for each angle, the silhouettes were aligned using the pot as invariant element of the images.

**Target Shape And Offset Computation** The largest internal circle that fitted the untrimmed bush was computed for each image. From the whole sequence of images the mean target radius of the untrimmed bush was computed as average of the radii of each fitted circle. Each largest internal circle was visually checked to evaluate the presence of incoherent fitting due to a wrong bush segmentation. The average radius was used to evaluate the performance instead of the radius of the fitted sphere delivered by the vision pipeline (see Section 2.1.6) due to problems that arose during the tests (see Secion 2.3.2).

From the mean target circle obtained, a ring was calculated (see Figure 8) with external radius equal to target sphere radius plus 20 mm and the internal equal to the radius minus 20 mm (see Section 2.3.1).

Furthermore, the bush centroid of was computed as average of the fitted circles centers.

 

Figure 7: Preprocessed image of untrimmed bush with the manually segmented landmarks for Normalized Cross Correlation (NCC) rigid registration algorithm (left); The extrapolated landmarks used as model for the registration (center); Preprocessed image of trimmed bush after the rigid registration (right)

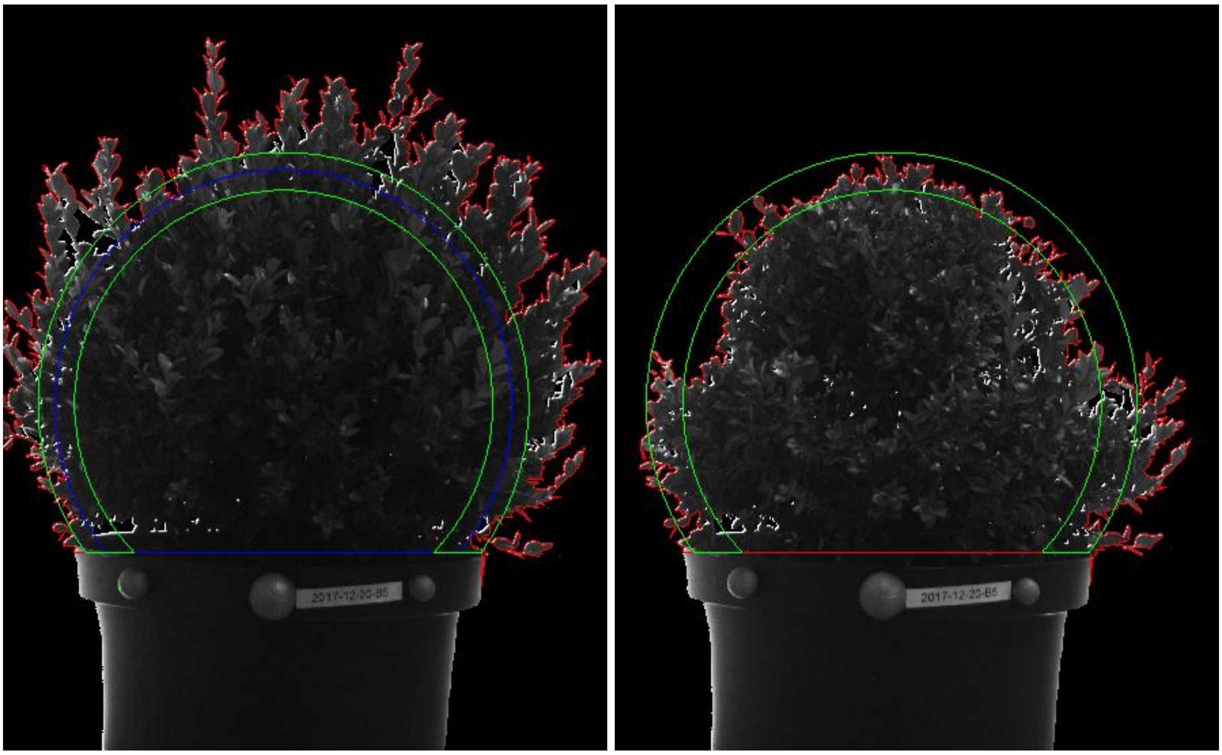


Figure 8: Computed ring from the largest fitted circle on the segmented bush (left); Ring projection on the trimmed bush silhouette (right).

**Trimming Accuracy Test** Using the computed ring the amount of pixels inside and outside of the ring per each picture was computed. For the pixels that have fallen inside the ring the correspondent region was classified as *correctly trimmed* (see Figure 9); if they were outside the external circle the region was classified as *poorly trimmed*; finally if the there were holes in the silhouette inside the internal circle the correspondent part of region was classified *deep trimmed*.

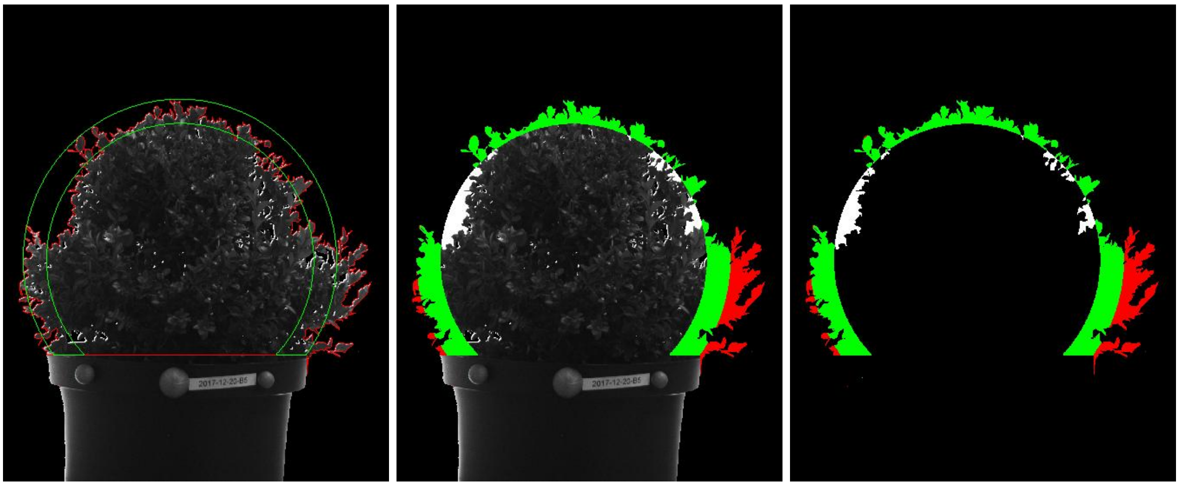

Figure 9: Trimmed bush with projected ring (left); computation of the correct, poor, and deep trimmed surfaces of the bush (center); in the image only the correct (green), poor (red), and deep trimmed (white) pixels are shown (right)

To correctly evaluate the trimming performance, the target shape computed on the untrimmed bush has to be correctly projected on the trimmed one. To assure the correct projection the misalignment between each untrimmed and trimmed bush has to be calculated and corrected. Considering the pot center as invariant, for each registered picture of both the untrimmed and trimmed bush the offset $\xi$ between the pot center and the center of circle fitted to the extrapolated untrimmed bush was computed (see Figure 10). Furthermore the offset $\Psi$ between the center of the pot and the rotation axis of the rotation table was computed. After trimming, the offset $\Psi'$ between the untrimmed-bush-pot-center and the trimmed-bush-pot-center was computed. Considering the offset $\vartheta = \Psi + \Psi' + \xi$ for each picture the target shape was correctly projected on the trimmed bush.

The trimming performance is computed as average over all the pictures of the sequence of the difference of the outgrown region of bush before the trimming pixels and the poorly trimmed region:

$$TP = \sum_{j=0^\circ}^{359^\circ} \frac{C_{or_j} - C_{pt_j}}{C_{or_j}} \tag{1}$$

where $TP$ is the percentage of the trimming performance; $C_{or_j} = \sum_{i=1}^{outsidering} p_{or_{ij}}$, represents the pixels outside the external circle before the trimming action i.e. the outgrown region; $C_{pt_j} = \sum_{k=1}^{outsidering} p_{pt_{kj}}$ represents the pixels outside the external circle after the trimming i.e. the poorly trimmed region. If the poorly trimmed region is zero, TP is 100%; if the poorly trimmed region is equal the outgrown region, TP is 0%.

However, $TP$ is not enough to describe the trimming performance quality because it does not take into account the deep trimmed regions.

 

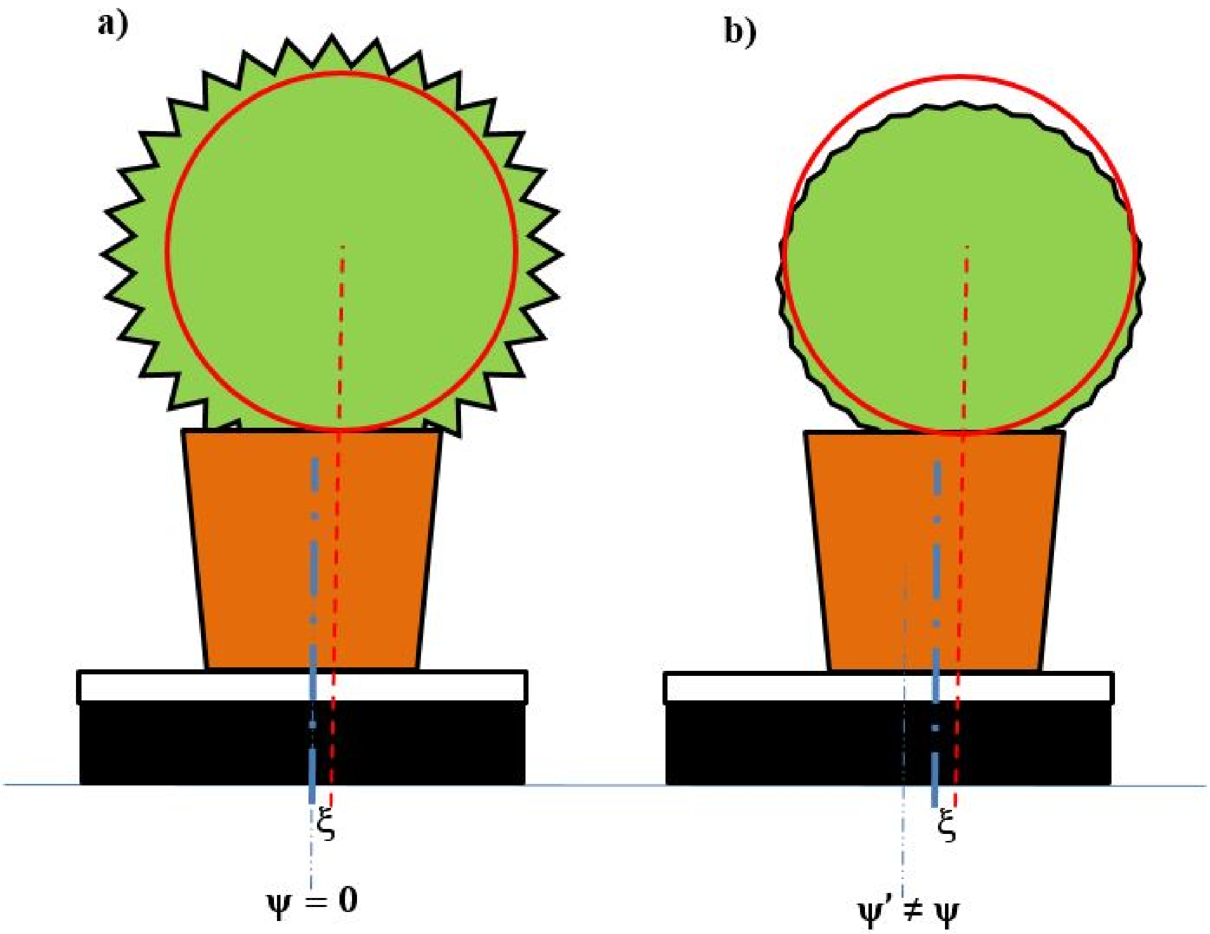


Figure 10: Schematic overview of bush-center-pot-center offset of the untrimmed bush and relative projection of target shape: for simplicity the offset $\Psi$ between center of the pot and rotation table axis is zero (left); projection of the target shape on the trimmed bush after the untrimmed-trimmed-pot-center offset calculation (right).

To quantitatively evaluate the quality of the trimming performance the amount of pixels present in one of the regions described above was given in percentage relatively to the total amount of pixels computed, i.e.

$$CT = \sum_{j=0^\circ}^{359^\circ} \frac{C_{ct_j}}{C_{ct_j} + C_{pt_j} + C_{dc_j}} \tag{2}$$

$$PT = \sum_{j=0^\circ}^{359^\circ} \frac{C_{pt_j}}{C_{ct_j} + C_{pt_j} + C_{dc_j}} \tag{3}$$

 

$$DT = \sum_{j=0^\circ}^{359^\circ} \frac{C_{dt_j}}{C_{ct_j} + C_{pt_j} + C_{dc_j}} \tag{4}$$

where $CT$, $PT$, and $DT$ are the percentage of the correctly trimmed, poorly trimmed, and deep trimmed bush surface, respectively; $C_{ct_j} = \sum_{i=1}^{ring} p_{ct_{ij}}$, $C_{pt_j} = \sum_{i=1}^{outsidering} p_{pt_{ij}}$, and $C_{dt_j} = \sum_{i=1}^{insidering} p_{dc_{ij}}$ represent the pixels inside the three different areas.

**Symmetry Test** To evaluate the symmetry of the trimmed bush, we mirrored, for each image, the left half of the segmented bush along the axis passing the bush centroid (see Figure 11). Then the intersection $A_{mirrored} \cap A$ between the left and the right half image of the bush was computed.

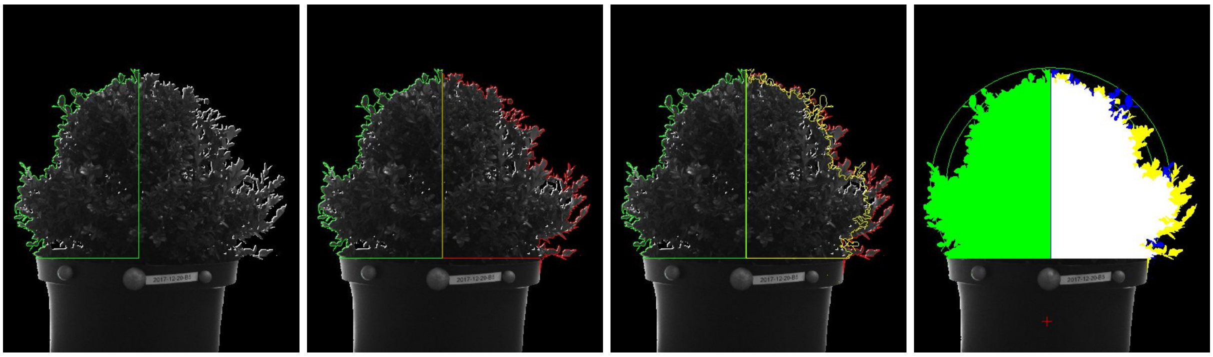

Figure 11: Definition of the left half of the segmented bush silhouette (green delineation) (left); definition of the right half binary image (red delineation) ($2^{nd}$ left); mirrored left part on the right part (yellow delineation) ($2^{nd}$ right); intersection of the two half's (white area) (right).

Using the Dice Similarity Coefficient (DSC) [3] (see Equation 5) the similarity between the two half's can be computed.

$$DSC = \frac{2|A_{mirrored} \cap A|}{|A_{mirrored}| + |A|} \tag{5}$$

$DSC$ is the Dice similarity coefficient and ranges between 0 and 1. Furthermore the sum of absolute value of the two half's $|A_{mirrored}| + |A|$ is, in this case, the whole bush.

### 2.1.6 Bush Evaluation Procedure

Before the trimming test, each bush was put on the turntable of the evaluation rig (Section 2.1.4) and a sequence of images was automatically acquired (Section 2.1.5). Then the white reflection screen was removed and the test rig was moved to its fixed test location (Section 2.1.1). During the trimming test, ROSbags of the robot and camera activities were recorded.

To automatically activate the open loop motion planning process the software described in Deliverable 2.2 was implemented in a Finite State Machine using FlexBE ROS application (see Figure 12)

 

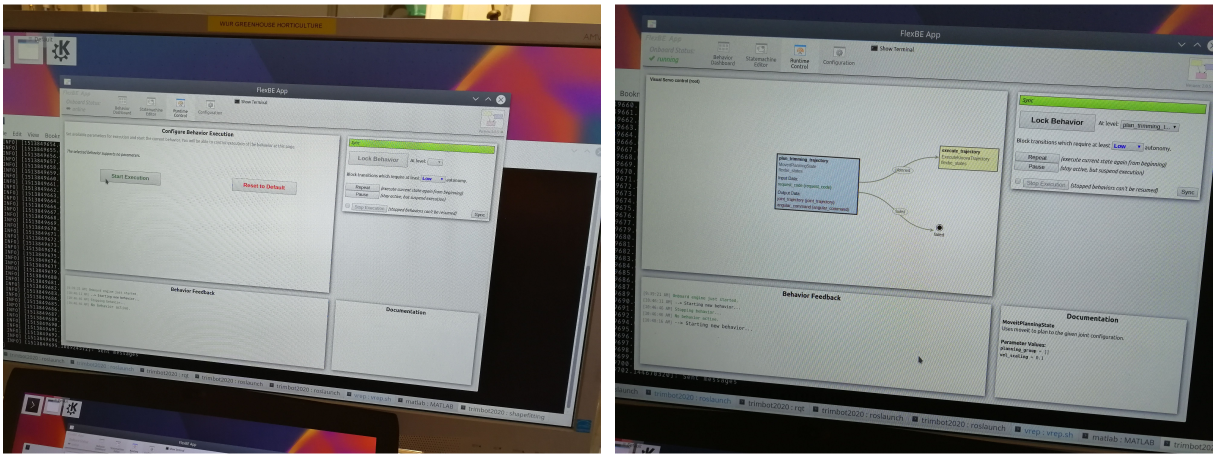


Figure 12: Start procedure for the motion planning (left). Computed plan trimming trajectory state (right).

Using the vision pipeline described in the Deliverable 2.2[1] an image of the bush is taken by the stereo camera system mounted on the end-effector (Section 2.1.2) and the motion plan is calculated. This was designed to cover $\frac{1}{5}$ of the total bush surface. An example of trimming action is shown in Figure 13.

When the robot had completed the trimming of the reachable surface, the turntable was automatically activated and the bush was rotated 72° and the trimming was repeated with the same motion plan.

After the complete bush rotation, the test rig was removed and the white reflection screen was set back in its position, the back illumination was switched and a new sequence of evaluation images was automatically taken.

Using the analysis software described in Section 2.1.5 the difference between bush shape before and after the trimming, and between the trimmed shape and the target shape were evaluated (see Section 2.2).

During the trimming action, movies were taken to visually evaluate the quality of bush trimming end-effector and the motion planning.

## 2.2 Results

The execution time to complete the trimming process was obtained from the ROSbag registrations and was around 16 minutes, i.e. 3 minutes and 20 seconds per each surface trimming (see Section 2.1.6).

The trimming bush performance, in percentage, is given in Table1 together with percentage of corrected, poor, and deep trimming quality.

The values are given as the average per each bush over the whole sequence of acquired and registered images.

Figure 13: The robot in trimming action on a $\frac{1}{5}$ of the total bush surface.

Table 1: Overview of the bush trimming test result for all the bushes

| Bush n. | Trimming performance | Correct trimming | Poor trimming | Deep trimming |
|---|---|---|---|---|
| B1 | 75% | 61.2% | 38% | 0.8% |
| B2 | 77.3% | 49.8% | 33% | 17.2% |
| B3 | 85% | 43.4% | 26% | 30.6% |
| B4 | 89% | 49.3% | 21% | 29.7% |
| B5 | 82% | 49.8% | 29.2% | 21% |

One example image before and after the trimming test is given in Figure 14. Examples of the first acquired image before and after the trimming test for each bush are given Figure 22 in the Appendix (Section A).

The average of the target radii computed by the evaluation software system are shown in Table 2 together with the best target radii delivered by the vision pipeline. From the findings it is possible to observe that the two sets of radii are comparable but the radii computed by the evaluation software system were more stable and coherent, e.g. bush B4 in Table 2 (see Section 2.1.5).

The evaluation results of the bushes surface symmetry after the trimming are shown in Table 3. From

 


Figure 14: Preprocessed image of the untrimmed bush number 4 (left); silhouette of the untrimmed bush number 4 ($2^{nd}$ left); preprocessed image of trimmed bush number 4 ($2^{nd}$ right); silhouette of trimmed bush number 4 (right)

Table 2: Overview of the target radii delivered by the vision pipeline and the radius averages computed by the evaluation software for each bush over all rotation pictures. For the visual pipeline target radius there were some incoherent results, e.g. bush B4

| Bush n. | Visual pipeline target radius | Evaluation method mean target radius |
|---|---|---|
| B1 | 32 cm | 31 cm |
| B2 | 30 cm | 29 cm |
| B3 | 30 cm | 30 cm |
| B4 | 38 cm | 30 cm |
| B5 | 30 cm | 30 cm |

the results it is possible to see that the trimmed bushes present an high DSC score due to the bush rotation during the trimming process.

Table 3: Overview of the Dice Similarity Coefficient (DSC) index

| Bush n. | Mean DSC | standard deviation DSC |
|---|---|---|
| B1 | 0.91 | 0.02 |
| B2 | 0.88 | 0.03 |
| B3 | 0.90 | 0.01 |
| B4 | 0.92 | 0.03 |
| B5 | 0.89 | 0.03 |

From the movies taken during the trimming action (see Section 2.1.6) the qualitative analysis of the arm motion revealed that many no-trimming actions were taken. These occurred due to the singularities of the manipulator during the execution of the coverage trajectory (Deliverable [1]).

Due to the anisotropic growth of the bushes (see Section 2.1.3) some branches presented an angle of incidence with the rotation blades smaller that 30°. This is due to the chosen strategy that requires a tangent attitude of the blades to the bush surface. Moving the end-effector down-up, the blades push some of the branches inwards without cutting them.

 

## 2.3 Discussions and Conclusion

### 2.3.1 Specifications

From the Trimbot2020 project specifications (see Deliverable 7.3[6]), a bush has to be trimmed with an accuracy of ±5 mm. However, while executing the experiments described here, it was observed that this accuracy is not realistic due to the accuracy performance of the Kinova Jaco[2] robot arm, the compliant bush surface and mechanical constraints of the robotic arm and the end-effector. For these reasons we tested the bush trimming defining an accuracy of ±20 mm, see Figure 15.

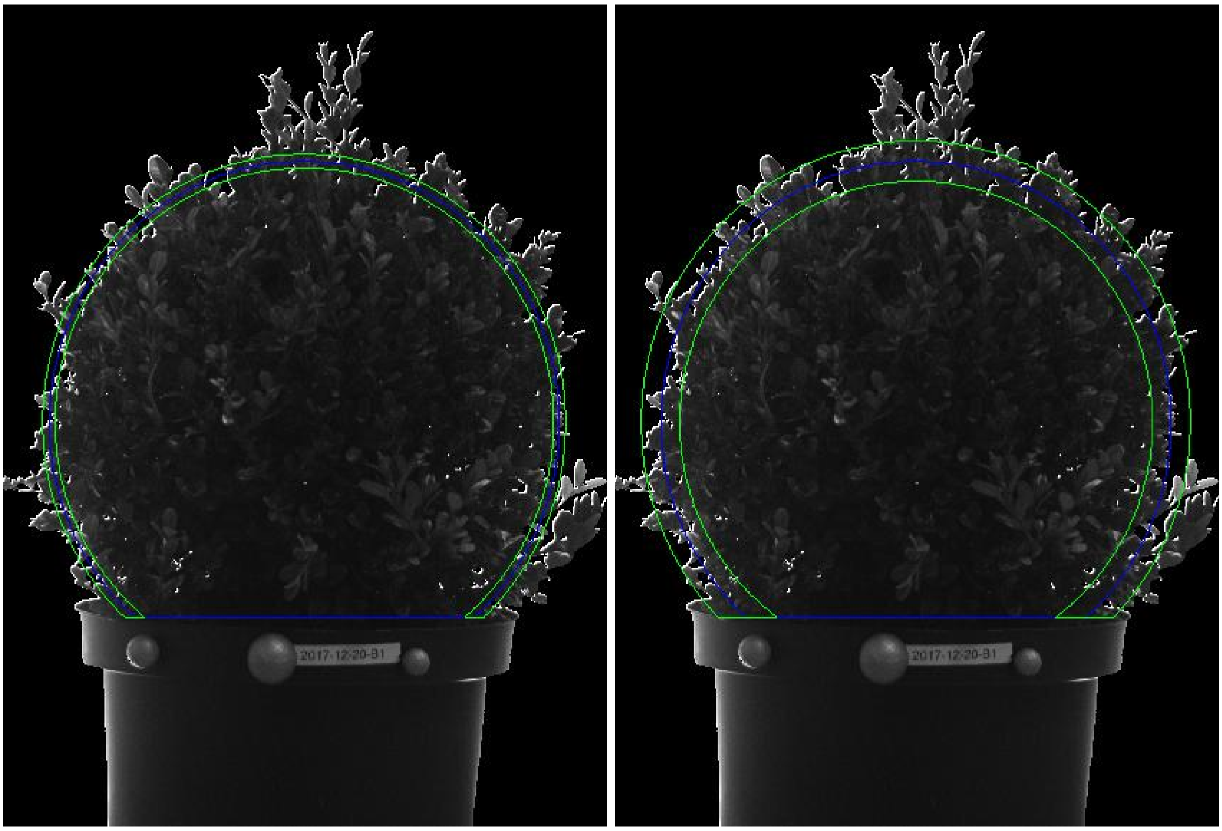

Figure 15: trimmed bush number 1 with the projected target shape (blue circle) and the ±5 mm accuracy ring (left); bush number 1 with ±20 mm ring accuracy (right)

### 2.3.2 Vision Pipeline

During the tests the target sphere computed by the vision pipeline (Deliverable 2.2[1]) was not stable and the values were incoherent (see Table 1) because the fitting process[4] of the calculated shape to the observed bush was inaccurate. This is due to the fact that the fitting algorithm, used for the target shape computation, was performed using only one image taken from stereo camera set-up a short distance and from that pose less than 50% of the bush can be seen. To use multiple viewpoints is ongoing work and will be implemented.

 

One of the main effects was that during the test it was very difficult to produce a reliable target sphere shape. This reduced the trimming performance (see Section 2.3.3) because with the implemented open loop motion planning was not possible to adjust the coverage trajectory planning.

Therefore, for the validation, the target has been recomputed using a largest fitted circle inside the bush extrapolated from each silhouette (see Section 2.1.5).

### 2.3.3 Untrimmed Outgrown Branches

The performance of bush trimming was lower than the requirements: on average only 82% of total outgrown branches were trimmed instead of 95%. However, most of the poorly trimmed branches were located close to the edge of the pot. This is due to the manipulator's geometrical constraints for reachability and dexterity at the ground combined with the dimensions of camera set-up that limits the manipulator's collision free workspace. During the test performed in the lab, the ground level was defined at pot edge; consequently the robot could not reach those branches.

Furthermore, due to anisotropic growth of the bushes combined with chosen end-effector attitude respect to the bush surface (see Section 2.2), the end-effector down-up motion was, sometimes, not effective.

Only 51% of the trimming runs had a precision better than 20 mm: in four cases the robot trimmed too much of the bush. Only the very first bush presented a very low percentage of too deep trimming, however, also a poor trimming performance on the top of the bush was present due to an error of the motion plan coverage. The main reason of this was that the target sphere fed to the motion plan calculation was too small.

### 2.3.4 Camera Set-up

Some weak points in the end effector design popped out when, during the bush trimming evaluation session, the camera set-up touched in some occasions the bushes.

The main issue is that the temporary mechanical set-up, combined with the position and dimensions of the camera's together with the bulky presence of the FPGA is prone to misalignments (and miscalibrations) of the camera set-up in case of accidental collisions.

A second important issue is that the dimensions of the actual set-up limit the reachability and dexterity of the manipulator especially when the end-effector is close to the ground because they decrease the manipulator collision free workspace.

Furthermore, the stereo camera set-up is not protected by a housing; during the tests, after a collision with the bush, a camera broke down, as shown in Figure 16.

Finally the camera flat cables to the FPGA are exposed and they can be easily broken or pulled off.

 

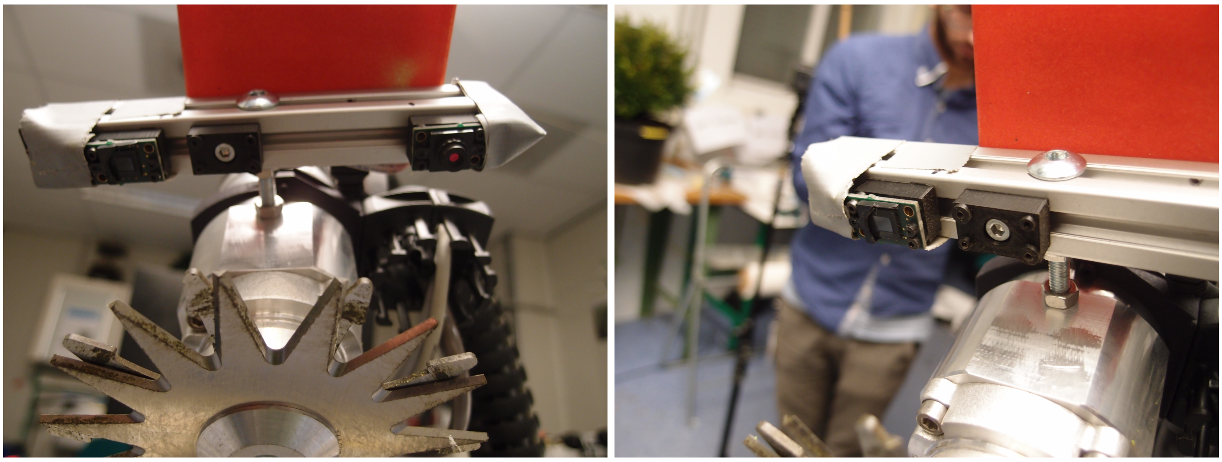

Figure 16: Broken camera

#### 2.3.5 Recommendations for Bush Trimming

From the experience gained during the test session, the following recommendations are given:

- A new design of the set-up is needed to protect the camera and avoid misalignments between the stereo set-up and the end-effector.
- To enhance the collision free workspace the dimensions of the end-effector have to be reduced. To achieve this the FPGA has to be moved behind the motor and the camera pairs has to be set parallel to the motor axis.
- The use of a composite point cloud generated by multiple images acquired along a dedicated robot trajectory to produce a better bush fitting.
- The requirements about the bush trimming accuracy have to be reconsidered.
- Motion planning cost-function has to take in account for singularities of the manipulator to reduce the number of the no-trimming actions.
- The cutting strategy has to be modified for effective trimming of the anisotropic outgrowth of the bushes.

# 3 Rose Clipping Test

## 3.1 Materials and Methods

#### 3.1.1 Rose Clipping Test Rig

In order to evaluate the performance of the rose-cutting tool the same test rig was used (see Figure 17), as used for the bush trimming evaluation. Furthermore, since the rose plants are planted in the soil

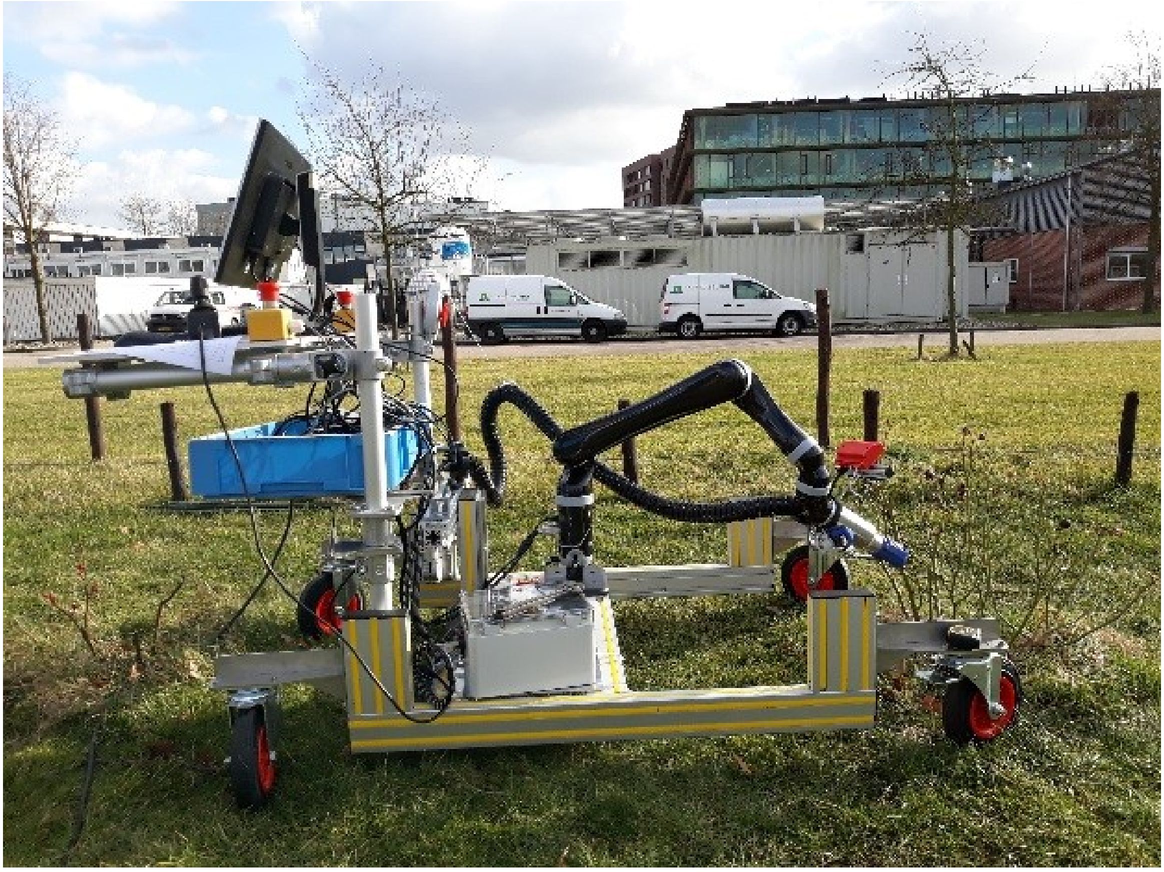

Figure 17: Complete system during rose clipping test.

the height of the arm base was adapted to match the height which is estimated to be used in the final system (Deliverable 1.2[5]).

### 3.1.2 Rose Clipping End-Effector

The tool which is evaluated is designed and built as described in Deliverable 2.2[1]. The cables from the control unit are guided via a cable-guide which was hanging next to the arm. Furthermore, a camera rig was mounted to fit 2 stereo camera pairs. The location was chosen in a way that the knife mechanism was in the field of view of the sensor (TCP in the FOV). The distance from the Camera to the TCP was maximized without interference with the robotic arm (190mm). This resulted in the camera setup seen in Figure 18.

### 3.1.3 Rose Clipping Evaluation Procedure

The performance of the rose clipping tool was determined by a practical field test. This test was performed on the 4 available rose bushes in the test garden at the Wageningen location. Based on the general rules of trimming of rosebushes the position and orientation of the optimal clipping point was determined. This resulted in the following set of rules (see Figure 19):

 

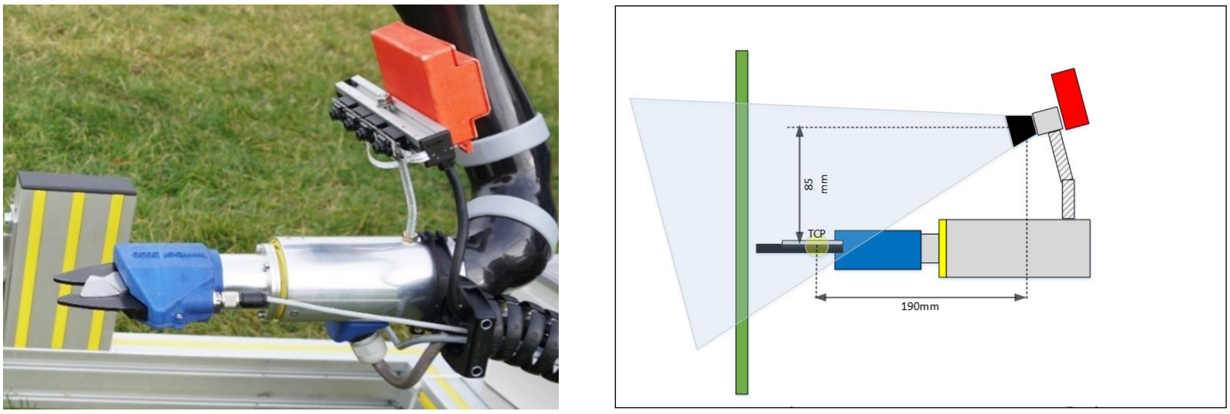


Figure 18: Rose cutting tool with camera's mounted on the robotic arm during the field test (left). Schematic overview of the rose cutting tool and the position of the camera's (right)

- Cut about $\frac{1}{2}$-1cm above the rose bud;
- cut in the plane 20-30° with a slope opposite of the rose bud;
- position determined by the desired shape of the rose (higher/lower, bud on inside or outside).

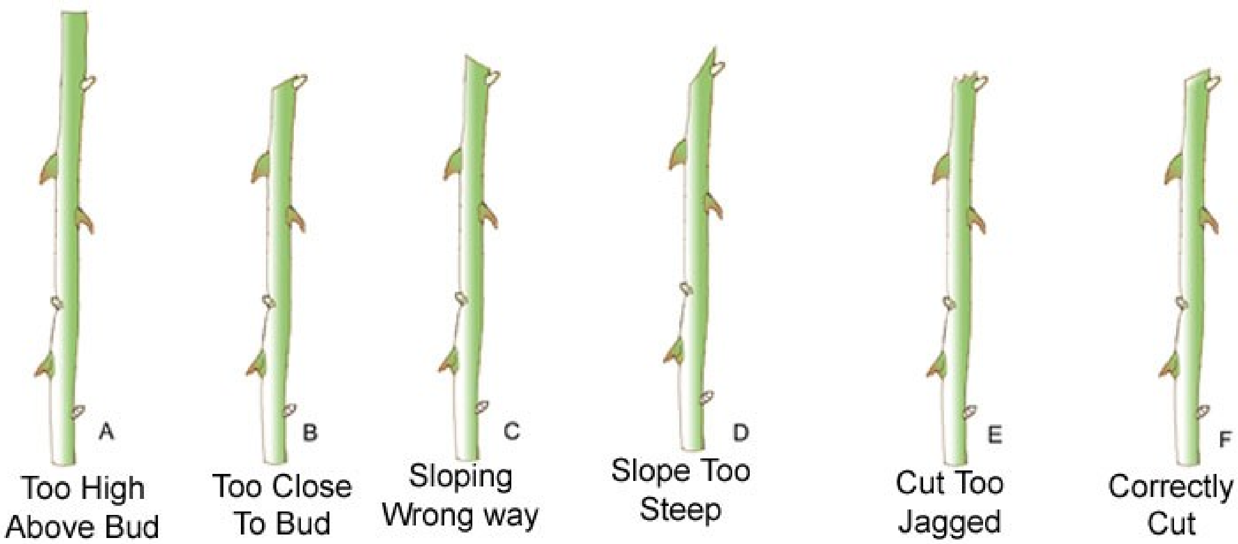


Figure 19: Practical general rules for rose pruning[1]

[1] https://www.thetreecenter.com/pruning-roses

The position of the bud, is determined by the shape you want the bush to grow. In order to cover a broad set of pruning strategies, the rosebud positions were randomly chosen, from high to low and from inside to outside facing buds.

The test rig platform was placed at a distance of about 75cm from the rose plant center, with the tool in retracted position (Figure 20a). From this point, all cutting points which were in reach were

 

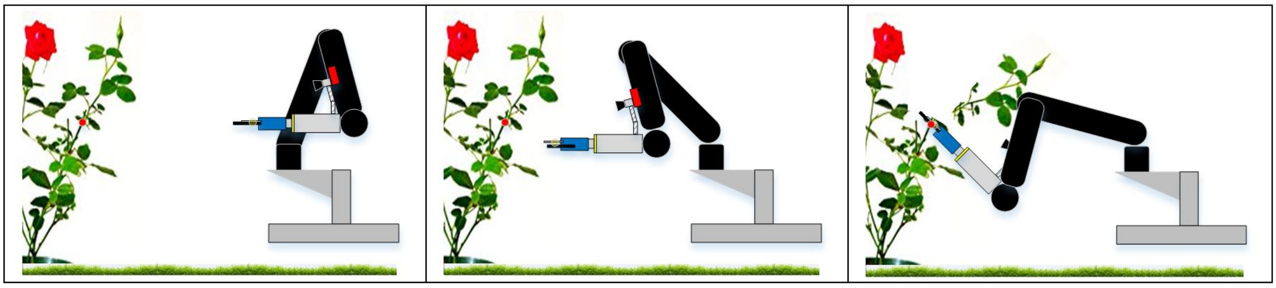

Figure 20: Approach action during a cutting attempt: start position with robot arm retracted and desired cutting point in red (a), tool approaching target (b), tool in desired orientation and position at which cutting action is performed (c)

attempted to trim. This means manually adapting the position and orientation till the knife has reached the optimal trimming point, mimicking a visual-servo-like movement (Figure 20b). While moving towards the trim position, ROSbags were recorded of the 2 stereo camera pairs. When the arm reached the trim location and orientation, the cutting action is performed (Figure 20c). Then the robot is moved back to the retraction position, and the performance indicators are noted. Furthermore, if the tool was not able to reach a specific orientation/position, the cause for this was noted. This gives an insight for the possible redesign/adaption of the current design.

The following parameters were noted:

- Rose number [-] $\rightarrow$ reference to specific plant in the garden (1-4).
- Height from the ground [cm] $\rightarrow$ height of the optimal clipping point.
- Horizontal distance from center plant [cm] $\rightarrow$ horizontal distance from optimal clipping point to center of the plant.
- Distance to robot base [cm] $\rightarrow$ horizontal distance from optimal clipping point to center of the robot.
- Angular error [°] $\rightarrow$ angular error between optimal orientation and actual cutting angle.
- Positional error [cm] $\rightarrow$ distance between the optimal cutting position and the actual cutting position.
- Reason for position error/angular error [-] $\rightarrow$ what stopped the robot from reaching the optimal cutting position.

## 3.2 Results

As shown in Table 4, 25 pruning attempts were evaluated. From these 25, one of them could not be reached due to reachability (singularity) of the arm. Furthermore at 6 of the 25 branches, the optimal cutting point and orientation could not be met within ±5mm from the optimal position or ±10° degree

Table 4: Overview of the field test result for all the branches

| Object | Rose n. | Diam. | Hight | Center dist | Platform dist. | Ang. err. | Pos. err. | Lim. ang/pos. | Cut. Qual. | Reason for not reaching optimal cutting point |
|---|---|---|---|---|---|---|---|---|---|---|
| 1 | 1 | 6 | 65 | 15 | 68 | 10 | 1 | False | 4 | |
| 2 | 3 | 6 | 56 | 30 | 79 | 10 | -1 | False | 4 | |
| 3 | 3 | 6.5 | 47 | 30 | 70 | 10 | -4 | False | 4 | |
| 4 | 3 | 5 | 58 | 10 | 83 | 0 | -4 | False | 5 | |
| 5 | 3 | 4 | 47 | 18 | 86 | 0 | -5 | False | 3 | Pushed to the stem → resulting not nice cut |
| 6 | 3 | 2.5 | 38 | 20 | 97 | - | - | False | - | Out or reach |
| 7 | 3 | 1.5 | 39 | 20 | 80 | 25 | 5 | True | 5 | Camera in bush |
| 8 | 3 | 5 | 44 | 5 | 78 | 10 | 3 | False | 5 | |
| 9 | 3 | 5 | 22 | 8 | 70 | 20 | 2 | True | 5 | Pushed a lot of branches |
| 10 | 3 | 8 | 21 | 0 | 70 | 0 | 0 | False | 5 | |
| 11 | 3 | 10 | 5 | 0 | 69 | 10 | -10 | False | 5 | No problems due to positive (upwards cutting angle from base) |
| 12 | 2 | 7 | 73 | 26 | 60 | 10 | 4 | True | 4 | Singularity |
| 13 | 2 | 14 | 12 | 7 | 70 | 0 | -4 | False | 4 | |
| 14 | 2 | 8 | 13 | 12 | 77 | 5 | 10 | False | 5 | |
| 15 | 2 | 7 | 19 | 12 | 73 | 0 | -5 | False | 3 | |
| 16 | 2 | 9 | 20 | 15 | 68 | 5 | 2 | False | 1 | Pushed to the stem → resulting not nice cut |
| 17 | 2 | 4 | 19 | 12 | 83 | 15 | 21 | True | 5 | Pushed a lot of branches |
| 18 | 4 | 7 | 24 | 6 | 70 | 5 | 1 | False | 4 | |
| 19 | 4 | 6 | 21 | 8 | 78 | 0 | 11 | True | 5 | Camera in bush |
| 20 | 4 | 8 | 18 | 8 | 72 | 10 | -1 | False | 4 | |
| 21 | 4 | 5.5 | 22 | 7 | 68 | 10 | 1 | False | 5 | |
| 22 | 3 | 6 | 45 | 30 | 66 | 10 | 2 | False | 5 | |
| 23 | 3 | 5 | 40 | 13 | 80 | 10 | -5 | False | 4 | |
| 24 | 3 | 6 | 34 | 35 | 53 | 0 | 0 | False | 4 | |
| 25 | 3 | 8 | 16 | 10 | 83 | 15 | 0 | True | 5 | Tool/arm reached the ground level |
| **Min** | **1** | **1.5** | **5** | **0** | **53** | **0** | **-10** | | **1** | |
| **Max** | **4** | **14** | **73** | **35** | **97** | **25** | **21** | | **5** | |

from the optimal position. As shown above the main reasons for not reaching the cutting point were the tool dimensions, which could not fit in the complex plant structure. Furthermore the cameras mounting (and FPGA box) reduced reachability when they were pushing to other stems. Also in one case the tool was too long, with the result that the tool hit the ground (Figure 21). However, it must be mentioned that during this experiment only the reachable buds from one position were evaluated. From other platform positions it might be possible to cut the remaining branches. The cutting quality was overall fine, except some exceptions when the stem was pushed, which resulted in bad cutting quality.

 

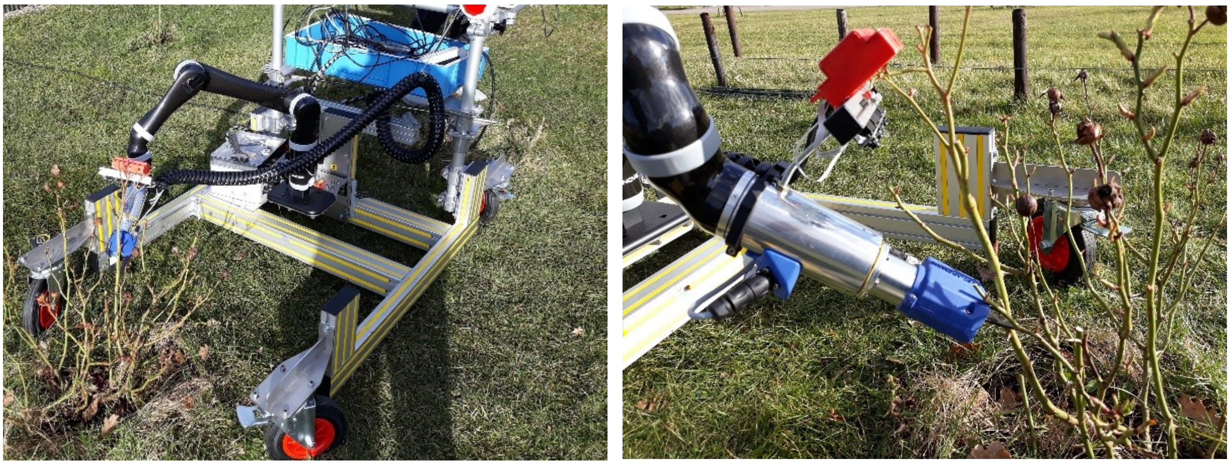

Figure 21: Overview of complete system with the rose clipping tool at desired cutting point (left). FPGA housing stuck against plant branches (right).

### 3.3 Discussion and Conclusion

Overall, the performance of the system is good. In the end 24 of 25 positions (96%) were able to cut. And 18 of the 24 positions (75%) were reached without any limitations in orientation or position. Furthermore, since the buds were only attempted from 1 position, the performance could be increased if one cutting position was attempted from multiple base positions. Furthermore, due to the manual control during this test, the position and orientation error was bigger than it is expected to be in automatic guidance.

The cutting quality is in most cases good, even with branches of 14 mm diameter. In two cases the tool has pushed the to be cut branch, resulting in an unsmooth cut. This results in a tension on the branch, which causes the branch to partially break before cutting. An increase of speed of opening and closing of the knife (from 4 seconds to 2 seconds) might overcome this problem.

The length of the tool limits in some cases the reachability (1 out of 25). When the desired cutting point on the plant is already low, the tool sometimes needs to be pushed down in the ground due to the yaw angle for cutting. However this can be overcome by reaching the stem from another orientation in the same plane.

The sensor location was fine for visual control of the gripper. However it was a big obstacle in terms of reachability. Especially the camera FPGA (red box) on the backside needs to be put closer to the motor housing. Furthermore the dimensions of aluminium frame which carries the sensors itself needs to be minimized, to maximize reachability.

One aspect to consider is that the rosebud will always be on the bottom of the tool. When the cameras are on the top side of the tool, this means the last part of the trajectory there is no updated information about the location of the bud. However, facing the camera upwards will cause a lot of lightning issues, so it will be a trade-off of the two.

 

### 3.3.1 Recommendations for Rose Clipping

The following recommendations for adaptations of the tool were generated based on this test:

- Reduction of the length of the tool, which will increase reachability and ability to cut at low positions from the ground.
- Location of the sensors is fine, but it is necessary to decrease their dimensions to mount them on the end-effector.
- Put FPGA of the camera at another location
- Increase speed of cutter to 2 seconds per cycle.

# References

[1] Wageningen Research (WR), Wageningen University (WU), Albert-Ludwigs-Universität Freiburg (ALUF). TrimBot2020 Deliverable D2.2: Manipulator and tools version 1, running Open-Loop Motion Planning.

[2] Lee Dah-Jye, Xiaoqian Xu, Joseph Eifert, and Pengcheng Zhan. Area and volume measurements of objects with irregular shapes using multiple silhouettes. Optical Engineering - OPT ENG, 02 2006.

[3] Lee R. Dice. Measures of the Amount of Ecologic Association Between Species. *Ecology*, 26(3):297–302, 1945.

[4] David Eberly. Least squares fitting of data. *Chapel Hill, NC: Magic Software*, 2000.

[5] Wageningen Research (WR), Wageningen University (WU), Robert Bosch GmbH (BOSCH). TrimBot2020 Deliverable D2.1: tate-of-the-art, progress beyond, and system design for mechatronics, motion planning and vision-based replanning.

[6] UEDIN. TrimBot2020 Deliverable D7.3: Component and System Evaluation Plan.

# A Bush Trimming Appendix

Examples of the first acquired image before and after the trimming test for each bush are given Figure 22.

 

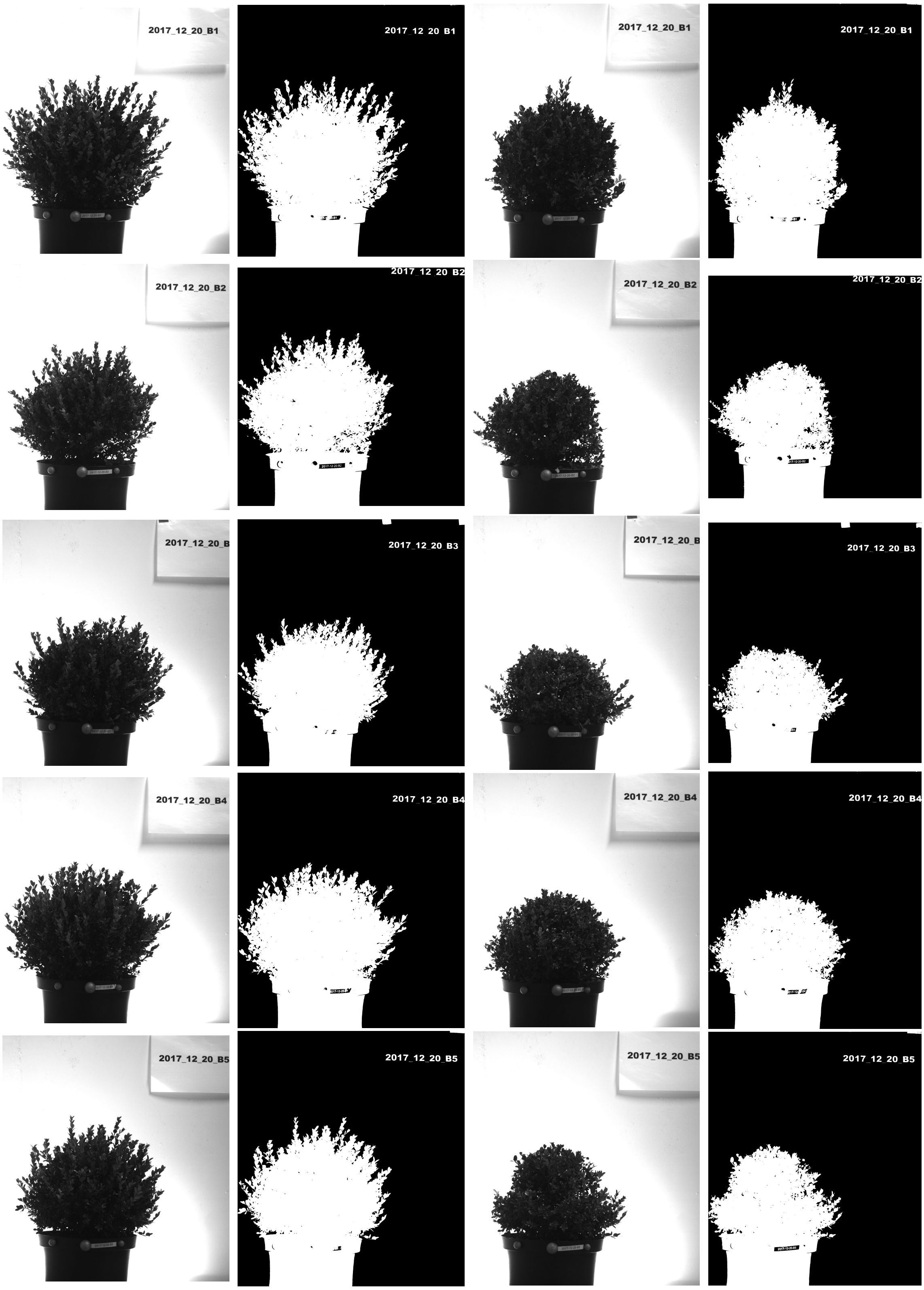


Figure 22: Preprocessed image of the untrimmed bush number 1-5 (left column); silhouette of the untrimmed bush number 1-5 ($2^{nd}$ left column); preprocessed image of trimmed bush number 1-5 ($2^{nd}$ right column); silhouette of trimmed bush number 1-5 (right column)